High Sensitivity Phonon Spectroscopy of Bose-Einstein Condensates using Matter-Wave Interference

N. Katz,[1] R. Ozeri,[1,*] J. Steinhauer,[1,†] N. Davidson,[1] C. Tozzo,[2,3] and F. Dalfovo[3,4]

[1]*Department of Physics of Complex Systems, Weizmann Institute of Science, Rehovot 76100, Israel*
[2]*Dipartimento di Fisica, Università di Trento, I-38050 Povo, Italy*
[3]*Istituto Nazionale per la Fisica della Materia, BEC-INFM Trento, I-38050 Povo, Italy*
[4]*Dipartimento di Matematica e Fisica, Università Cattolica del Sacro Cuore, Via Musei 41, 25121 Brescia, Italy*

(Received 5 May 2004; published 24 November 2004)

We study low-momentum excitations of a Bose-Einstein condensate using a novel matter-wave interference technique. In time-of-flight expansion images we observe strong matter-wave fringe patterns. The fringe visibility is a sensitive spectroscopic probe of in-trap phonons and is explained by use of a Bogoliubov excitation projection method applied to the rescaled order parameter of the expanding condensate. Gross-Pitaevskii simulations agree with the experimental data and confirm the validity of the theoretical interpretation. We show that the high sensitivity of this detection scheme gives access to the quantized quasiparticle regime.

DOI: 10.1103/PhysRevLett.93.220403 PACS numbers: 03.75.Kk, 03.75.Lm, 32.80.–t

The peculiar nature of a Bose-Einstein condensate (BEC) is clearly observed in its low-momentum excitations, revealing the many-body coherent nature of the system. Recent experiments have provided observations of the Bogoliubov excitation spectrum, superfluidity, and suppression of low-momentum excitations due to quantum correlations in the ground state [1–3].

In these experiments the condensates were typically excited by Bragg pulses [4] and imaged after a free expansion. At high momenta the excitations were clearly separated from the expanding condensate, and could be counted and quantified. Even in the phonon regime (wavelength larger than but comparable to the healing length) a well-defined excitation cloud could still be distinguished from the condensate [see Fig. 1(a)] and was found to be amenable to direct atom counting methods.

However, at sufficiently low momentum (wavelength much larger than the healing length), we observe a new regime, in which the excitations and the condensate no longer separate, regardless of the duration of the expansion. The excitations are manifested in a clear density modulation of the cloud in the absorption images [see Fig. 1(c)], reminiscent of *in situ* observations of low energy, zero momentum excitations of the condensate [5,6], but they differ significantly from these since they involve both nontrivial time-of-flight (TOF) dynamics and a small, but finite, excitation momentum.

In this Letter we analyze the dynamics of phonons in such freely expanding condensates using both the Gross-Pitaevskii equation (GPE) and a dynamically rescaled Bogoliubov theory [7]. We find that, in our elongated condensate, axial low-momentum phonons are adiabatically converted by the (mainly radial) expansion into free atoms with the same axial momentum. The overlap of these moving free particles with the expanding ground state results in the axial periodic density modulations observed in the TOF images.

We use the fringe visibility of these density modulations after TOF, as an extremely sensitive spectroscopic probe of the excitation strength. Whereas the sensitivity of atom or momentum counting methods [2] scales quadratically with the quasiparticle excitation amplitude, we show that the fringe visibility scales linearly with these amplitudes. This enhanced sensitivity was noted and used to estimate the degree of adiabaticity in the loading of a BEC into an optical lattice [8], but not as a spectroscopic probe of the excitations themselves.

Our nearly pure ($> 95\%$) ^{87}Rb condensate in the $|F, m_f\rangle = |2, 2\rangle$ ground state, is formed in an elongated

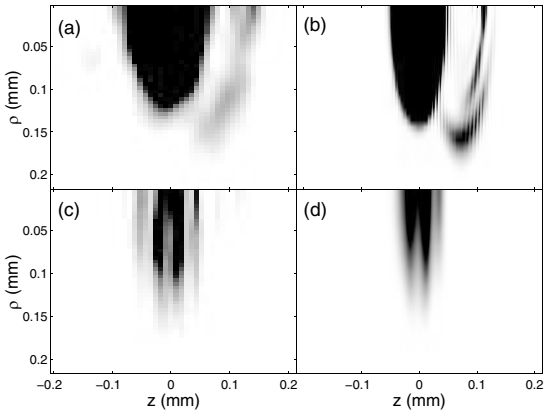

FIG. 1. Density $n(\rho, z)$ of the expanding condensate, initially excited with phonons of momentum q. In (a) and (b): $qa_\rho = 2.03$. The density in (a) is obtained by computerized tomography of TOF column density absorption images, $n_{\mathrm{col}}(y, z)$. In this image we measure nearly 2×10^4 excitations, while (b) corresponds to a full GP simulation. In both cases, note the clearly separated excitation cloud on the right of the condensate. The same quantities are plotted in (c) and (d) for $qa_\rho = 0.31$. Note the strong density modulation, with no significant outcoupled fraction. The number of excitations in the simulation is 9.6×10^2.

cylindrically symmetric harmonic trap with axial frequency $\omega_z = 2\pi \times 25$ Hz and radial frequency $\omega_\rho = 2\pi \times 220$ Hz. The radial harmonic oscillator length is $a_\rho = (\hbar/m\omega_\rho)^{1/2} = 0.73$ μm. We use condensates with $N = 10^5$ atoms, having chemical potential $\mu = \eta\hbar\omega_\rho$, with $\eta = 9.1$, and an average healing length $\xi \sim 0.3a_\rho$. Using Bragg excitation beams detuned 6.5 GHz above the $5S_{1/2}, F = 2 \rightarrow 5P_{3/2}, \quad F' = 3$ transition, Bogoliubov quasiparticles are excited in the condensate along the $\hat{z}$ axis, at a controlled wave number q by varying the angle between the two beams. At a given q the frequency difference between the beams ω is controlled via acousto-optic modulators. After the Bragg pulse (of duration $t_B = 6$ m sec) the magnetic trap is rapidly turned off and after 38 m sec of TOF an on-resonant absorption image is taken, with the absorption beam perpendicular to the $\hat{z}$ axis.

The dynamics of phonons within an expanding condensate has recently been studied [7] and shown that, within a short time interval ($t \sim \omega_\rho^{-1}$), phonons are converted into single particle excitations trraveling at an axial velocity of the order of $\hbar q/m$. This velocity should be compared to that of the slowly expanding axial boundary, which travels at the asymptotic velocity $\pi\omega_z^2 Z_{TF}/2\omega_\rho$, where $Z_{TF} = a_\rho(\omega_\rho/\omega_z)(2\eta)^{1/2}$ is the Thomas-Fermi axial radius of the condensate. Thus at long expansion times the excitations can separate out from the condensate only if $qa_\rho > q_c a_\rho = \pi(\omega_z/\omega_\rho)(\eta/2)^{1/2}$, while for $q < q_c$ they remain within the condensate at all times. For our experimental parameters we calculate $q_c a_\rho = 0.76$. Indeed, we begin to observe a distinct excitation cloud at $qa_\rho \simeq 0.72$. However, this transition is not sharp and a small fraction still overcomes the condensate boundary even at lower q. This escaped fraction was used to find the resonance in our previous measurement of the excitation spectrum [2].

In the phonon regime, but with $q > q_c$, using computerized tomography [9] [see Fig. 1(a)], the freely expanding excitation cloud was measured to be carrying almost all the momentum and excess energy of the system due to excitation. By solving the GPE for the TOF dynamics, we now confirm this experimental observation quantitatively for this regime. For instance, the lateral cloud in Fig. 1(b) carries about 99% of the momentum and more than 95% of the energy of the initial phonons. In Fig. 1(b) one also notices that the released cloud is radially wider than the condensate, in agreement with the experimental observation [9] and has an evident "shell structure." Both features are associated with the spatial structure of the Bogoliubov amplitudes of the in-trap initial excitations [7] and the presence of excitations with radial nodal lines. At this momentum ($qa_\rho = 2.03$) counting the population of the excitation cloud also gives reasonable agreement with the population expected by simple structure factor considerations [2].

Turning our attention to the very low-momentum excitations with $qa_\rho = 0.31$, we study the TOF density modulations of Figs. 1(c) and 1(d) in detail. Figure 2 shows the linear density of the expanded condensate, defined as $2\pi \int_0^\infty \rho n(\rho, z) d\rho$. We note a slight asymmetry to the right, which is related to the initial direction of propagation of the phonon [10].

To quantify the fringes of Fig. 1(c), we take the Fourier transform of the measured density profile, and observe clear sidelobes (Fig. 3). We define the fringe visibility as the area of the sidelobes divided by the area of the central lobe. This is a powerful "spatial lock-in" method to reduce noise in the measurement. We note the ease of the measurement, due to the clear separation between the Fourier peaks, despite the very low momenta involved. This should be contrasted with the atom counting methods, where it becomes increasingly difficult to discern the excitation cloud at finite expansion times in real space. At such low momentum we do not expect any significant radial excitations, due to negligible coupling to all higher radial modes [11,12]. This is confirmed by the lack of any features in the transverse direction in Figs. 1(c) and 3(a).

Figure 4 shows the fringe visibility as a function of the Bragg frequency detuning (circles). We find the resonances to be at $\pm 137 \pm 10$ Hz, which compares favorably with the expected value 138 ± 5 Hz for the average Bogoliubov frequency in local density approximation (LDA) [13]. The width of the resonances is due to the finite duration of the Bragg pulse.

A direct GPE simulation of the experiment (Fig. 4, solid line) gives good agreement with the observed data. However, little intuition is gained by this. Therefore, we also compare this spectrum to the analytic result obtained with a rescaled quasiparticle projection method [7] (dashed line).

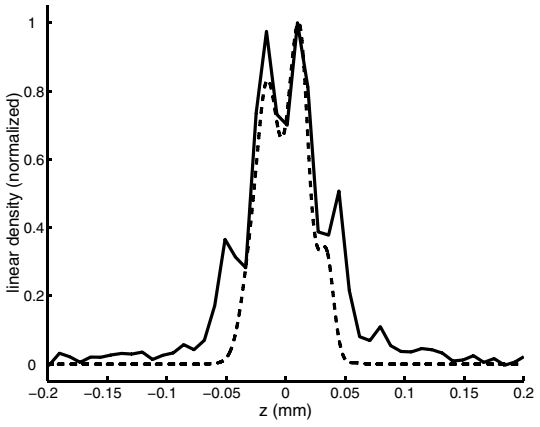

FIG. 2. Linear density $2\pi \int_0^\infty \rho n(\rho, z) d\rho$ measured from TOF image with very low-momentum excitation $qa_\rho = 0.31$ (solid line). Note the slight asymmetry to right, which is in agreement with the GPE simulation (dashed line).

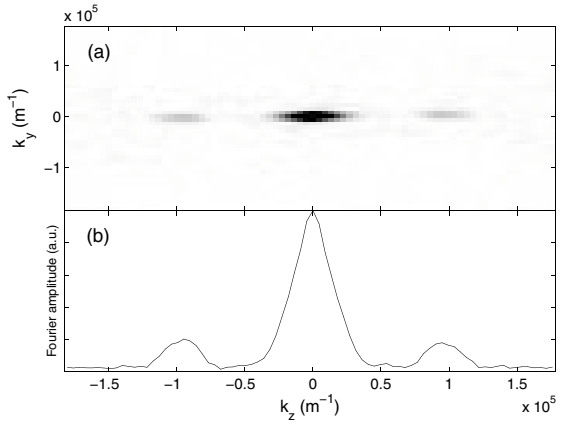

FIG. 3. Fourier transform of the column density $n_{\rm col}(y, z)$ for the same image as Fig. 1(c). (a) Fourier transform. (b) Integration over central strip of (a). Note the clear separation between the central mode and the sidelobes, despite the low-momentum of the excitation.

For this, we consider a uniform gas in a box of volume L^3, with a density $n_0 = N/L^3$. The ground state order parameter is $\Psi_0 = \sqrt{n_0}$, with chemical potential $\mu = g n_0$. The excited states are the well-known Bogoliubov quasiparticles, having frequency $\omega_k = \{k^2/(2m)[\hbar^2 k^2/(2m) + 2\mu]\}^{1/2}$ and amplitudes $u_k, v_k = \pm\{[\hbar^2 k^2/(2m) + 2\mu]/(2\hbar\omega_k) \pm 1/2\}^{1/2}$.

We insert the linear expansion

$$\Psi(z, t) = e^{-i\mu t/\hbar}\Big\{n_0^{1/2} + L^{-3/2}\sum_k c_k(t) u_k e^{i(kz-\omega_k t)} + c_k^*(t) v_k^* e^{-i(kz-\omega_k t)}\Big\} \quad (1)$$

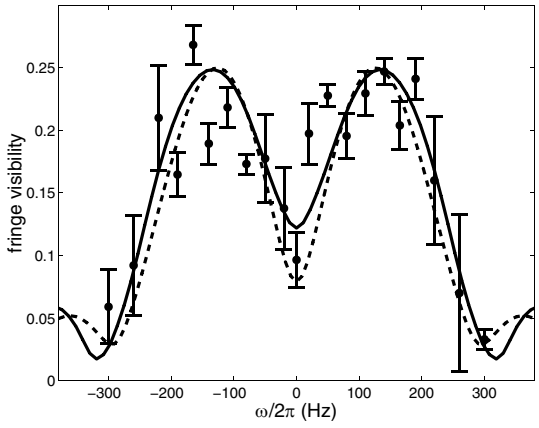

FIG. 4. Fringe visibility as a function of the Bragg excitation frequency (points). The error bars represent the uncertainty due to four measurements. We observe a clear double-peaked spectrum, which is finite-time broadened. The peaks are found at $\omega = \pm 137 \pm 10$ Hz, close to the expected Bogoliubov frequency (138 ± 5 Hz). The solid line is a full GPE simulation of the experiment. The dashed line is the result of Eq. (5).

into the GPE. The Bragg pulse is included through the potential $V = V_B \cos(qz - \omega t)$, acting for $-t_B < t < 0$. At $t = -t_B$ the condensate is assumed to be in the ground state, so that $c_k(-t_B) = 0$ for all k's. The equations for the coefficients $c_k(t)$ are then solved analytically [12,14]. After the Bragg pulse one gets

$$c_{\pm q}(0) = \mp \frac{V_B\sqrt{N}(u_q + v_q)}{2\hbar(\omega \mp \omega_q)}[e^{\pm i(\omega \mp \omega_q)t_B} - 1] \quad (2)$$

and $c_k(0) = 0$ for $|k| \neq q$.

Next we assume that the uniform gas undergoes a fictitious radial expansion which mimics the actual expansion, by taking a uniform time-dependent density that decreases in time as the average density of elongated condensate. For this we choose the density n_0 to be equal to the radial average of the density of a cylindrical condensate, $n_0 = (2/5)n(0)$, having the same central density $n(0)$ of our trapped condensate, and we treat the expansion by means of the scaling ansatz [15,16].

In this case, the density decreases as $n_0/b^2(t)$, where $b^2(t) = 1 + \omega_\rho^2 t^2$ is the radial scaling parameter. In the presence of quasiparticles with wave vector $\pm q$, one can write a rescaled order parameter $\tilde{\Psi}$ in the form

$$\tilde{\Psi}(z, t) = \tilde{\Psi}_0 + L^{-3/2}\sum_{k=\pm q} c_k(0)\tilde{u}_k(t)e^{ikz} + c_k^*(0)\tilde{v}_k^*(t)e^{-ikz}. \quad (3)$$

At $t = 0$, when $\tilde{u}_k(0) = u_k$, $\tilde{v}_k(0) = v_k$, and $\tilde{\Psi}_0 = \sqrt{n_0}$, this expression coincides with (1). At $t > 0$, $\tilde{\Psi}_0$ remains stationary while the quantities $\tilde{u}$ and $\tilde{v}$ are time-dependent amplitudes that obey rescaled Bogoliubov-like equations [7].

Further simplification is obtained by assuming adiabatic quasiparticle-to-particle conversion. This corresponds to assuming that, after an expansion time $t \gg \omega_\rho^{-1}$, the rescaled amplitude $\tilde{u}$ becomes unity, while $\tilde{v}$ vanishes [17]. In terms of $\tilde{\Psi}$, this implies

$$\tilde{\Psi}(z, t) \to \tilde{\Psi}_0 + L^{-3/2}[c_q(0)e^{iqz} + c_{-q}^*(0)e^{-iqz}]. \quad (4)$$

Since the expansion is assumed to be radial, the linear density obtained by radial integration of the rescaled density $|\tilde{\Psi}|^2$ coincides with that obtained from $|\Psi|^2$. The same is true for their Fourier components with $k = 0$ and $k = \pm q$. The sum of the $\pm q$ coefficients, divided by the $k = 0$ coefficient is exactly the visibility γ as defined for the experimental analysis. One finds $\gamma = (2/\sqrt{N}) \times |c_q(0) + c_{-q}^*(0)|$ or, recalling Eq. (2),

$$\gamma = \frac{V_B}{\hbar}\left[1 + \frac{4\mu m}{\hbar^2 q^2}\right]^{-1/4} \times \left|\frac{e^{i(\omega-\omega_q)t_B} - 1}{\omega_q - \omega} + \frac{e^{-i(\omega+\omega_q)t_B} - 1}{\omega + \omega_q}\right|. \quad (5)$$

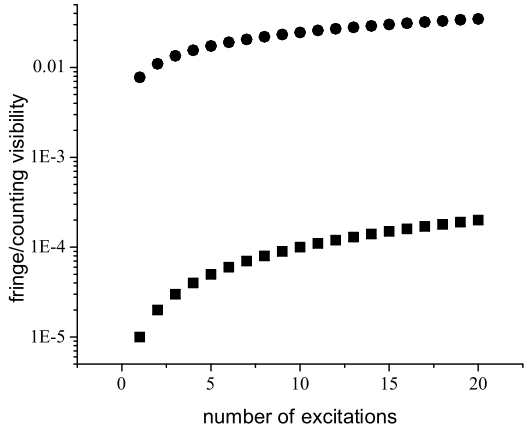

FIG. 5. Theoretical fringe visibility after TOF for $qa_\rho = 0.31$ (circles) compared with the standard atom counting technique for $qa_\rho = 2.03$ (boxes), as a function of the number of excitations. The visibility of the atom counting method grows linearly in excitation number with a very weak slope of $1/N$, whereas the fringe visibility is not negligible ($\sim 0.76\%$) even for a singly quantized excitation, and grows as the square root of the number of excitations.

The dashed line in Fig. 4 corresponds to this expression, calculated for the same V_B used in the GPE simulations ($V_B = 0.1\hbar\omega_\rho$) and with no fitting parameters. The agreement with both experiment and GPE simulation indicates that the essence of the release process of a BEC with such very low-momentum excitations is indeed captured by simply assuming that, due to the reduction of the average background density in which the excitations live, quasiparticles are adiabatically converted into free particles that interfere with the ground state.

We stress that, in this linear response analysis for $q < q_c$, the predicted fringe visibility is proportional to c_q, which is in turn proportional to $V_B(u_q + v_q)$. By measuring the fringe visibility at the different calculated excitation amplitudes of Fig. 4, we indeed find that a linear fit is much better than a quadratic one. Conversely, at higher momentum ($q > q_c$), the number of observed atoms in the excitation cloud is linear in the number of excitations, given by $|c_q|^2$, and quadratic in the quasiparticle amplitudes. This is also consistent with the results of our GPE simulations, where the fringe visibility at low q and the counting visibility at high q are found to be proportional to V_B and V_B^2, respectively.

In our experiments and simulations, we typically excite a few hundred quasiparticles (~ 1000 at the peak of Fig. 4 and ~ 20 at the wings). However, by extrapolating the expected fringe visibility to lower Bragg intensities, one finds that it remains sizable even in the range of single quantized excitations. We compare (see Fig. 5) the fringe visibility at $qa_\rho = 0.31$ (circles) with the counting visibility at $qa_\rho = 2.03$ (boxes) for our experimental parameters [18]. The fringe visibility at low q is predicted to be over 2 orders of magnitude more sensitive. This implies a sensitive heterodyne technique to observe few, and possibly single quasiparticle excitations.

In conclusion, we discuss and implement a novel fringe visibility technique to observe the *in situ* matter-wave interference of low-momentum excitations with the condensate. We measure the excitation spectrum with high resolution and analyze the possibility of singly quantized excitation detection with this technique.

This work was supported in part by the Israel Ministry of Science, the Israel Science Foundation, and the DIP Foundation.

*Current address: Time and Frequency Division NIST 325 Broadway Boulder, CO 80305, USA.
†Current address: Department of Physics, Technion–Israel Institute of Technology, Technion City, Haifa 32000, Israel.

[1] D. M. Stamper-Kurn *et al.*, Phys. Rev. Lett. **83**, 2876 (1999).
[2] J. Steinhauer *et al.*, Phys. Rev. Lett. **88**, 120407 (2002).
[3] W. Ketterle and S. Inouye, C. R. Acad. Sci., Ser. IV **2**, 339 (2001).
[4] J. Stenger *et al.*, Phys. Rev. Lett. **82**, 4569 (1999); **84**, 2283 (2000).
[5] M.-O. Mewes *et al.*, Phys. Rev. Lett. **77**, 988 (1996).
[6] D. S. Jin *et al.*, Phys. Rev. Lett. **77**, 420, (1996).
[7] C. Tozzo and F. Dalfovo, Phys. Rev. A **69**, 053606 (2004)
[8] J. Hecker Denschlag *et al.*, J. Phys. B **35**, 3095 (2002).
[9] R. Ozeri *et al.*, Phys. Rev. Lett. **88**, 220401 (2002).
[10] We note a discrepancy in the axial size of the expanded condensate as compared to the GPE results, probably due to experimental imperfections in the release process, which is also present for unexcited condensates. The effect on the experimental observables is negligible.
[11] J. Steinhauer *et al.*, Phys. Rev. Lett. **90**, 060404 (2003).
[12] C. Tozzo and F. Dalfovo, New J. Phys. **5**, 54 (2003).
[13] A. Brunello *et al.*, Phys. Rev. A **64**, 063614 (2001).
[14] P. B. Blakie, R. J. Ballagh, and C.W. Gardiner, Phys. Rev. A **65**, 033602 (2002).
[15] Y. Kagan, E. L. Surkov, and G.V. Shlyapnikov, Phys. Rev. A **54**, 1753(R) (1996);**55**, 18(R) (1997).
[16] Y. Castin and R. Dum, Phys. Rev. Lett. **77**, 5315 (1996).
[17] In the case of the expanding homogeneous gas model adiabaticity has been shown to fail for $qa_r < q_a a_r \sim \eta^{-1/2}$ [7], corresponding to $qa_r < 0.3$. However, numerical analysis of the expanding inhomogeneous system indicates that adiabaticity fails only at an even lower q.
[18] The counting visibility is defined as the average momentum per atom in units of that of a single excitation, and is determined by the entire cloud density distribution after TOF.